Barchan dunes on bidispersed granular beds

C. A. Alvarez[1,2], F. D. Cúñez[1], E. M. Franklin[1]

[1]School of Mechanical Engineering, UNICAMP - University of Campinas,
Rua Mendeleyev, 200, Campinas, SP, Brazil
[2]Department of Atmospheric and Oceanic Sciences, University of California, Los Angeles,
Los Angeles, CA 90095-1565, USA

Key Points:

- Bidispersed grains segregate over barchan dunes with one species covering most of its surface
- A transient line, transverse to the flow direction, forms and migrates over the dune surface while segregation occurs
- We propose that the transverse line results from a competition between fluid entrainment and easiness of rolling

Corresponding author: Erick M. Franklin, `erick.franklin@unicamp.br`

Abstract

Barchans are dunes of crescentic shape found on Earth, Mars and other celestial bodies, growing usually on polydispersed granular beds. In this Letter, we investigate experimentally the growth of subaqueous barchans consisting of bidispersed grains. By tracking barchans in a water channel, we found that the grain distribution within the dune changes with the employed pair, and that a transient stripe appears on the dune surface, transverse to the flow direction, which we propose to be the result of a competition between the strength of fluid entrainment and easiness of rolling for each grain type. Our results provide new insights into barchan structures found in other planetary environments.

Plain Language Summary

This paper is devoted to crescent-shaped dunes, known as barchans, consisting of bidispersed grains. Barchans are found on Earth, Mars and other celestial bodies, with roughly the same morphology but different scales. Taking advantage of the much smaller and faster scales of subaqueous barchans (decimeter and minute, respectively), we performed experiments in a water channel where we obtained the evolution of barchan morphology and the motion of individual grains over the barchan surface. We found surface structures not still reported for aeolian barchans, but similar to those found on Mars at much larger and slower scales (kilometer and millennium, respectively), and explain their formation based on the motion individual grains. Our results open new possibilities to explain surface structures observed on Mars and other planetary environments.

1 Introduction

Barchan dunes, or simply barchans, are crescent-shaped dunes with horns pointing downstream that are frequently found on Earth, Mars and other celestial bodies (Bagnold, 1941; Herrmann & Sauermann, 2000; Hersen, 2004; Elbelrhiti et al., 2005; Claudin & Andreotti, 2006; Parteli & Herrmann, 2007; Courrech du Pont, 2015). They are formed under one-directional flows and limited amount of available grains and, under these conditions, present a robust shape that arise in diverse environments with a large range of scales, going from the kilometer and millennium in the case of Martian dunes down to the centimeter and minute in the aquatic case (Hersen et al., 2002; Claudin & Andreotti, 2006).

Because of their ubiquitous nature, barchans have been studied by using field measurements both on Earth (Finkel, 1959; Long & Sharp, 1964; Norris, 1966; Hesp & Hastings, 1998; Sauermann et al., 2000; Yang et al., 2019) and Mars (Breed et al., 1979; Schatz et al., 2006; Bishop, 2007; Bourke, 2010; Chojnacki et al., 2015; Runyon et al., 2017), which usually involve large time and length scales and uncontrolled conditions, producing valuable data that increased our understanding of many aspects of barchan morphodyamics, though with limited applicability for bedform evolution over long times and very few information at the grain scale. Given the smaller and faster scales of subaqueous barchans, experimental investigations were carried out in water channels and tanks under controlled conditions, from which it was possible to obtain the initial and long-time evolutions of the barchan morphology (Hersen et al., 2002; Alvarez & Franklin, 2017) and the motion of individual grains on the barchan surface (Alvarez & Franklin, 2018, 2019; Wenzel & Franklin, 2019). However, although natural beds are composed of polydispersed grains (Bagnold, 1941; Finkel, 1959; Long & Sharp, 1964), previous experiments investigated barchans of monodispersed particles, the only bidisperse-related references being the experiments of Caps and Vandewalle (2002) and Rousseaux et al. (2004) for size segregation within two-dimensional ripples and those of Groh et al. (2011) for density segregation within two-dimensional dunes.

Variations in the morphology and structure of barchans have been observed in nature, and in some cases have been described as resulting from hilly terrains (Finkel, 1959; Bourke, 2010; Parteli et al., 2014), wind changes (Finkel, 1959; Bourke, 2010; Parteli et al., 2014), barchan collisions (Long & Sharp, 1964; Hersen & Douady, 2005; Bourke, 2010; Vermeesch, 2011; Parteli et al., 2014; Assis & Franklin, 2020), or diverse processes over long time scales (Day & Catling, 2018). On Mars, barchan-shaped pits with stripes transverse to the flow direction were observed, which Day and Catling (2018) recently associated with dune casts formed by basalt flooding in ancient past and filled more recently with other sediments. Also on Mars, dunes with regions of different color, sometimes over the dune surface and other times on peripheral regions, were observed on its north pole and have been associated with the presence of coarse-grained ice together with sandy sediments (Breed et al., 1979; Schatz et al., 2006; Feldman et al., 2008; Ewing et al., 2010; C. J. Hansen et al., 2011; C. Hansen et al., 2013; Portyankina et al., 2013; Pommerol et al., 2013). For the latter dunes, the presence of two species with different sizes and densities could induce concentration of one of the species around the barchans, or induce segregation in horizontal layers. However, the precise organization of grains in those two-species barchans remains unknown.

In this Letter, we investigate experimentally the growth of subaqueous barchans consisting of bidispersed grains. We carried out exhaustive measurements where two-species barchans, in terms of grain sizes and/or densities, were tracked, and we varied the grain properties (size and density), their concentrations, and the water flow rate. We found that, while the barchan morphology remains roughly constant, denser, smaller, and smaller and less dense grains tend to accumulate on the barchan surface. For higher concentrations of the species accumulating on the surface, the other one forms a bottom layer and appears in top-view images as being around the barchan. We also found the appearance of a transient line on the dune surface, transverse to the flow direction, that forms during the growth of the single barchan, upstream its crest, and migrates toward the leading edge until disappearing. When grains of different densities but same size are used, that line consists of a large transverse stripe of different color. For the other pairs, that line consists in a transverse line that clearly separates a downstream region were segregation is complete from an upstream one where segregation is ongoing. The appearance of that transient line is intriguing, and we propose that it is the result of a competition between the strength of fluid entrainment and easiness of rolling for each grain type. For grains of different sizes, we observe, when the transient is finished, the presence of oblique stripes of much smaller wavelength than the dune size, which we associate with size segregation.

2 Materials and Methods

The experimental device consisted of a water reservoir, two centrifugal pumps, a flow straightener, a 5-m-long closed-conduit channel of transparent material and rectangular cross section (width = 160 mm and height 2δ = 50 mm), a settling tank, and a return line. The last 2 m of the channel consisted of the 1-m-long test section followed by a 1-m-long section discharging in the settling tank. With the channel previously filled with water, mixtures of grains were poured inside, forming an initial pile of conical shape that was deformed afterward into a barchan dune by imposing a turbulent water flow. We used different grain sizes and densities that were mixed by pairs in different concentrations, and we varied the water flow rate. A camera placed above the channel acquired images of the bedforms, from which measurements at both the dune and grain scales were obtained by image processing (Alvarez & Franklin, 2017, 2018, 2019; Alvarez, 2020; Kelley & Ouellette, 2011; Crocker & Grier, 1996; Cúñez & Franklin, 2020), while a camera placed horizontally acquired side-view images used for measurements of the dune height. With this technique, we had access to the granular structure over the barchan surface, but not to its inner structure. Figure 1a shows a picture of the test section, and a lay-

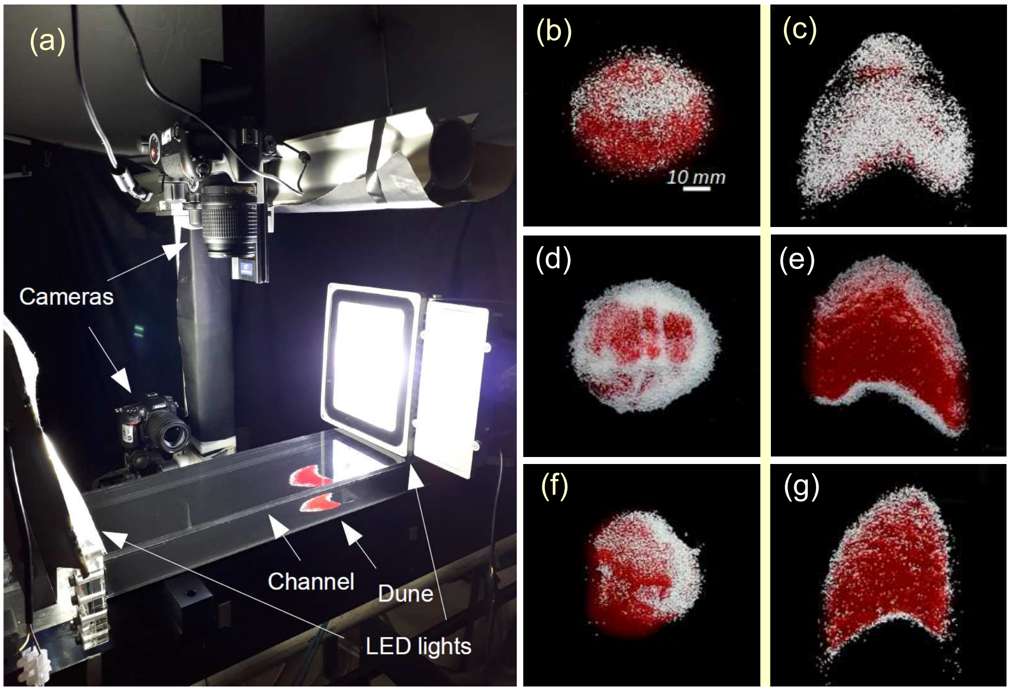

Figure 1. (a) Photograph of the experimental setup showing the test section, cameras, LED lights and dune. (b) and (c) Top views of the initial pile and barchan dune, respectively, for case e of Table 1 (different densities and same diameter); (d) and (e) initial pile and barchan dune, respectively, for case h of Table 1 (same density and different diameters); (f) and (g) initial pile and barchan dune, respectively, for case q of Table 1 (different densities and diameters). In Figures (b) to (g), flow is from top to bottom.

out of the experimental device and details about the used cameras are available in the supporting information.

Case ···	ϕ_1 ···	ϕ_2 ···	ϕ_3 ···	red ···	Re ···	d_{ratio} ···	$\rho_{s,ratio}$ ···	m_0 (g)
a	0.8	0.2	0	S_2	1.47×10^4	1	1.64	15.5
b	0.5	0.5	0	S_2	1.47×10^4	1	1.64	13.7
c	0.2	0.8	0	S_2	1.47×10^4	1	1.64	11.8
d	0.8	0.2	0	S_2	1.82×10^4	1	1.64	15.5
e	0.5	0.5	0	S_2	1.82×10^4	1	1.64	13.7
f	0.2	0.8	0	S_2	1.82×10^4	1	1.64	11.8
g	0	0.8	0.2	S_3	1.47×10^4	2.5	1	10.5
h	0	0.5	0.5	S_3	1.47×10^4	2.5	1	10.5
i	0	0.2	0.8	S_3	1.47×10^4	2.5	1	10.5
j	0	0.8	0.2	S_3	1.82×10^4	2.5	1	10.5
k	0	0.5	0.5	S_3	1.82×10^4	2.5	1	10.5
l	0	0.2	0.8	S_3	1.82×10^4	2.5	1	10.5
m	0.8	0	0.2	S_3	1.47×10^4	2.5	1.64	15.5
n	0.5	0	0.5	S_3	1.47×10^4	2.5	1.64	13.7
o	0.2	0	0.8	S_3	1.47×10^4	2.5	1.64	11.8
p	0.8	0	0.2	S_3	1.82×10^4	2.5	1.64	15.5
q	0.5	0	0.5	S_3	1.82×10^4	2.5	1.64	13.7
r	0.2	0	0.8	S_3	1.82×10^4	2.5	1.64	11.8

Table 1. Label of tested cases, initial concentration (volume basis) of each species within the initial pile, species with red (darker) color, channel Reynolds number *Re*, ratio between grain diameters d_{ratio}, ratio between grain densities $\rho_{s,ratio}$, and mass of the initial heap m_0.

The tests were performed with tap water at temperatures between 21 and 25 ^{o}C and three populations of particles were used: round zirconium beads (grain density ρ_s = 4100 kg/m^3) with grain diameters within 0.40 mm $\leq d \leq$ 0.60 mm, round glass beads (ρ_s = 2500 kg/m^3) with 0.40 mm $\leq d \leq$ 0.60 mm, and round glass beads with 0.15 mm $\leq d \leq$ 0.25 mm, which we call species 1, 2 and 3 (S_1, S_2 and S_3), respectively, and for which ϕ_1, ϕ_2 and ϕ_3 are the used concentrations (see supporting information for microscopy images of the used grains). For each dune, grains of different species had either white or red colors in order to track their distribution over the barchan dune. The cross-sectional mean velocities of water U were 0.294 and 0.364 m/s, corresponding to Reynolds numbers based on the channel height, Re $= \rho U 2\delta/\mu$, of $1.47{\times}10^4$ and 1.82×10^4, respectively, where ρ is the density and μ the dynamic viscosity of the fluid. The shear velocities on the channel walls u_* were computed from velocity profiles measured with a two-dimensional particle image velocimetry device (2D-PIV), and were found to follow the Blasius correlation (Schlichting, 2000). By using the hydraulic diameter of the channel, u_* is found to be 0.0168 and 0.0202 m/s for the two flow rates employed, corresponding to variations of Reynolds numbers at the grain scale, Re$_* = \rho u_* d/\mu$, within 3 and 10 and to Shields numbers, $\theta = (\rho u_*^2)/((\rho_s - \rho) g d)$, within 0.02 and 0.14, where we considered the midrange mean of the diameter of each species and g is the acceleration of gravity. All initial heaps had a volume of 7.0 cm^3, with initial masses varying between 10.5 and 15.5 g. The tested conditions are summarized in Table 1, where d_{ratio} and $\rho_{s,ratio}$ are the ratios between grain diameters and densities, respectively (see supporting information for values of Re$_*$ and θ and pictures of initial and final bedforms for each test).

3 Results

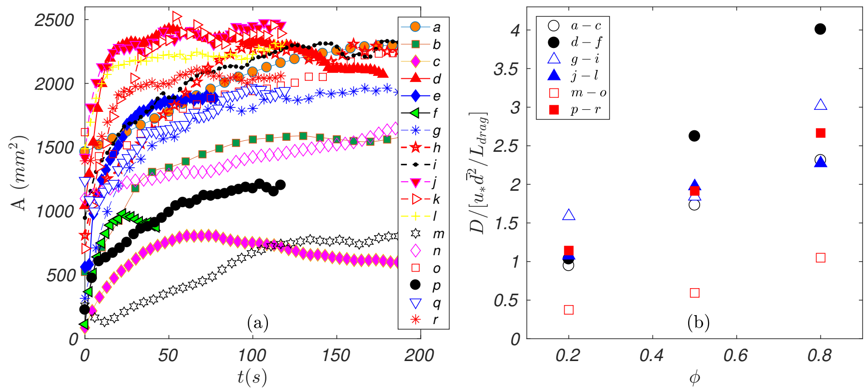

Figure 2. (a) Projected area A of the dune occupied by the species accumulating over its surface as a function of time. Cases c and m had their time scale multiplied by 0.65 and 0.35, respectively, in order to fit the graphic. (b) Normalized diffusion-like coefficient D as a function of the concentration ϕ of the species accumulating over the surface. Cases are listed in the key.

The general aspects of our results are summarized in Figures 1b to 1g. For different mixtures, grains segregate forming two main layers, one over the other, where the top layer consists of (i) denser grains when different densities are used (Figures 1b and 1c); (ii) smaller grains in the case of different diameters (Figures 1d and 1e); and (iii) smaller and less dense grains for different diameters and densities (Figures 1f and 1g). Those results are surprising, different gradings having been reported in the literature. For different sizes, cases g to r of Table 1, measurements on two-dimensional subaqueous ripples (Caps & Vandewalle, 2002; Rousseaux et al., 2004) showed that larger grains tend to accumulate over their crest, while coarse sediments form a bottom layer that remains immobile in the case of river dunes (Kleinhans, 2004). In the present case, although forming a bottom layer, coarse grains are periodically entrained by the fluid flow. For grains of different densities and same size, cases a to f of Table 1, a startling result had already been found by Groh et al. (2011) for two-dimensional dunes, where denser particles were found to accumulate in the central body of the dune, close to its top but covered by a thin layer of less dense grains. An explanation for that grading covered by a thin layer remains missing, and now we found something still different in the case of barchans. In the present case, we propose, based on Makse (2000), that the observed grading is the result of a competition between grains more easily entrained by the fluid flow and those that roll more easily over the bed.

In order to evaluate the segregation in horizontal layers, we analyzed the increase in the area occupied by grains accumulating over the dune surface. Figure 2a shows the projected area A of the dune (top view) occupied by the species accumulating over its surface as a function of time, for all the tested conditions, and it is a measure of the spreading of those species over the surface. Figure 2a shows the existence of an initial phase, in which spreading over the surface is occurring at a roughly constant rate, and a final phase, reached when the quantity of grains of each species over the surface remains roughly constant. Although grains are entrained by the fluid, we associate the spreading of grains over the surface with a diffusion-like mechanism, in a similar way as in the turbulence viscosity (Schlichting, 2000). For that, we defined a diffusion coefficient D (mm^2/s), given by the slope of initial phases of each curve in Figure 2a, and which we expect to scale, as shown in Eq. 1, with the inertial length for the stabilization of sand flux (Hersen et

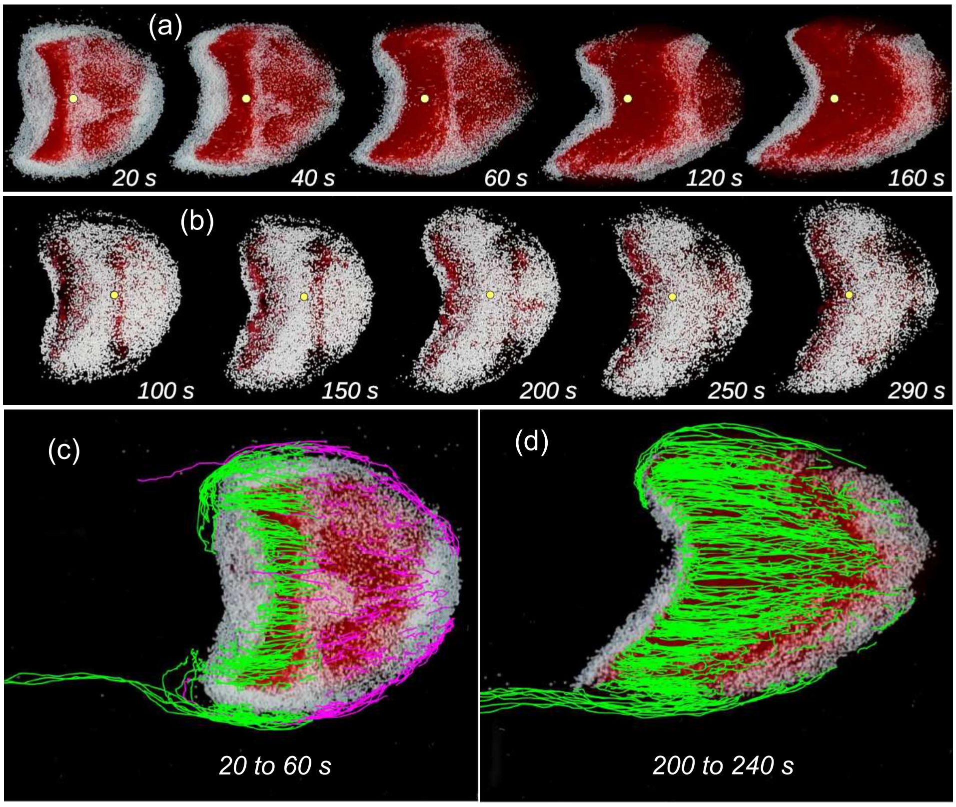

Figure 3. Evolution of the transverse stripe and trajectories of grains. (a) and (b) Snapshots of barchans at different instants showing the transverse stripe as it migrates to the leading edge. They correspond to cases h and b of Table 1, respectively, and the yellow circle indicates the crest position. (c) and (d) Trajectories of larger grains of case h, for two different intervals: when the stripe was still present and when it had already vanished, respectively. Trajectories were computed over 40 s and are superposed with the bedform image at the initial time of their computation. In Figure (c), green lines correspond to grains that started moving in positions downstream the transverse stripe, while magenta lines correspond to those that started moving in positions upstream the stripe.

al., 2002) $L_{drag} = (\bar{\rho}/\rho)\bar{d}$, the shear velocity u_*, and the mean diameter weighted by concentrations $\bar{d} = \left(\frac{\phi_a}{d_a} + \frac{\phi_b}{d_b}\right)^{-1}$, where $\bar{\rho} = \phi_a\rho_a + \phi_b\rho_b$, and a and b correspond to each species. Figure 2b presents $D\left(u_*\bar{d}^2/L_{drag}\right)^{-1}$ as a function of particle concentration for all tested cases, for which we obtain diffusion-like coefficients of the same order of magnitude, around unity. Although there is some variation, a diffusion-like coefficient seems proper for predicting the transient duration for the spreading of a species over the dune surface.

$$D \sim \frac{u_*\bar{d}^2}{L_{drag}} \tag{1}$$

The general structures observed over barchans after segregation has taken place can be better understood from the transverse line that forms on the dune surface during the growth of the single barchan and migrates toward the leading edge until disappearing. The evolution of the transverse stripe is shown in Figure 3 together with trajectories of larger grains migrating over the dune. Despite showing only some trajectories in Figures 3c and 3d, they represent well the behavior of the whole set. During the transient, we can observe a region where segregation has already occurred, downstream the transverse line, where larger grains (in cases of bidispersed size) and lighter grains (in the case of bidespersed density) flight over longer distances arriving directly on the crest and lee face, while the same does not occur on the region upstream the transverse line. In the latter region, segregation occurs faster close to the transverse line, where larger (cases g to r) or lighter (cases a to f) grains hop to the already segregated surface, and from there roll/flight easier over the smaller grains (in cases of bidispersed size). With that process, while larger or lighter grains travel to the lee face and form a carpet for the smaller ones, as proposed by Groh et al. (2011) in the 2D case, the line is displaced toward the leading edge until segregation is complete. When grains of different densities but same size are used, that line consists of a large transverse stripe of different color, and is similar to structures observed on Mars, though the proposed mechanisms and origins found in the literature are different (Day & Catling, 2018). In our experiments, the origin of the transverse stripe is always close to the crest of the initial pile, downstream of which segregation occurs fast due to the formation of a recirculation region and lee face, and from that position it propagates upstream with respect to the dune.

Finally, we observed also the presence of oblique stripes with wavelengths scaling with the grain diameter, as can be observed in the upstream region of the dune shown in Figure 1e. Based on images of cases g, h, j and k, we computed the arithmetic mean of wavelengths of oblique stripes, λ, 20 s after the transverse stripe had vanished, and found values of the order of $10d$ ($12 \leq \lambda/d \leq 16$, see supporting information for more images showing the oblique stripes and a table with λ for each case measured). It is difficult to explain their formation without measuring the inner grading of barchans; however, we speculate that their origin is a size segregation similar to those found in avalanches (Makse et al., 1998), but with the driving force in the direction of water streamlines.

4 Conclusions

In conclusion, we observed a general segregation with one particular species covering most of the dune surface. This segregation could be at the origin, together with solidification and frosting (as proposed by C. J. Hansen et al. (2011); C. Hansen et al. (2013); Portyankina et al. (2013); Pommerol et al. (2013)), of part of the structures observed on barchans on the north pole of Mars, for which top-view images show that dunes consisting of coarse-grained ice together with other sandy sediments present one species sometimes over the dune surface and other times on peripheral regions. We observed also a transient line on the dune surface, transverse to the flow direction, that migrates toward the leading edge, and that, when grains of different densities but same size are used, consists of a large transverse stripe. Similar stripes are found on barchan-shaped pits observed on Mars, resulting, however, from a different process (Day & Catling, 2018). We propose that the transverse line, as well as the segregation in horizontal layers, are the result of a competition between the strength of fluid entrainment and easiness of rolling for the involved species. These findings open new possibilities to explain surface structures observed on Mars and shed light on the barchan dynamics over polydispersed beds.

Acknowledgments

C. A. Alvarez is grateful to SENESCYT (Grant No. 2013-AR2Q2850) and to CNPq (Grant No. 140773/2016-9), F. D. Cúñez is grateful to FAPESP (Grant No. 2016/18189-0), and E. M. Franklin is grateful to FAPESP (Grant No. 2018/14981-7) and to CNPq (Grant No. 400284/2016-2) for the financial support provided. Data

supporting this work are available in the supporting information and in Mendeley Data (https://data.mendeley.com/datasets/z42c97sw4c).

References

Alvarez, C. A. (2020). *Genesis and formation of subaqueous barchan dunes : from a morphological characterization to a description at the grain scale.* Unpublished doctoral dissertation, University of Campinas. Retrieved from http://repositorio.unicamp.br/jspui/handle/REPOSIP/343638

Alvarez, C. A., & Franklin, E. M. (2017, Dec). Birth of a subaqueous barchan dune. *Phys. Rev. E*, *96*, 062906. Retrieved from https://link.aps.org/doi/10.1103/PhysRevE.96.062906 doi: 10.1103/PhysRevE.96.062906

Alvarez, C. A., & Franklin, E. M. (2018, Oct). Role of transverse displacements in the formation of subaqueous barchan dunes. *Phys. Rev. Lett.*, *121*, 164503. Retrieved from https://link.aps.org/doi/10.1103/PhysRevLett.121.164503 doi: 10.1103/PhysRevLett.121.164503

Alvarez, C. A., & Franklin, E. M. (2019, Oct). Horns of subaqueous barchan dunes: A study at the grain scale. *Phys. Rev. E*, *100*, 042904. Retrieved from https://link.aps.org/doi/10.1103/PhysRevE.100.042904 doi: 10.1103/PhysRevE.100.042904

Assis, W. R., & Franklin, E. M. (2020). A comprehensive picture for binary interactions of subaqueous barchans. *Geophys. Res. Lett.*, *47*(18), e2020GL089464.

Bagnold, R. A. (1941). *The physics of blown sand and desert dunes.* London: Chapman and Hall.

Bishop, M. A. (2007). Point pattern analysis of north polar crescentic dunes, mars: A geography of dune self-organization. *Icarus*, *191*(1), 151 - 157.

Bourke, M. C. (2010). Barchan dune asymmetry: Observations from Mars and Earth. *Icarus*, *205*(1), 183 - 197.

Breed, C. S., Grolier, M. J., & McCauley, J. F. (1979). Morphology and distribution of common sand dunes on Mars: Comparison with the Earth. *J. Geophys. Res.-Sol. Ea.*, *84*(B14), 8183-8204.

Caps, H., & Vandewalle, N. (2002). Patterns in hydraulic ripples with binary granular mixtures. *Physica A*, *313*(3), 357-364.

Chojnacki, M., Johnson, J. R., Moersch, J. E., Fenton, L. K., Michaels, T. I., & Bell, J. F. (2015). Persistent aeolian activity at endeavour crater, meridiani planum, mars; new observations from orbit and the surface. *Icarus*, *251*, 275 - 290.

Claudin, P., & Andreotti, B. (2006). A scaling law for aeolian dunes on Mars, Venus, Earth, and for subaqueous ripples. *Earth Plan. Sci. Lett.*, *252*, 20-44.

Courrech du Pont, S. (2015). Dune morphodynamics. *C. R. Phys.*, *16*(1), 118 - 138.

Crocker, J. C., & Grier, D. G. (1996). Methods of digital video microscopy for colloidal studies. *J. Colloid Interf. Sci.*, *179*(1), 298 - 310. Retrieved from http://www.sciencedirect.com/science/article/pii/S0021979796902179 doi: https://doi.org/10.1006/jcis.1996.0217

Cúñez, F. D., & Franklin, E. M. (2020). Crystallization and jamming in narrow fluidized beds. *Phys. Fluids*, *32*(8), 083303.

Day, M. D., & Catling, D. C. (2018). Dune casts preserved by partial burial: The first identification of ghost dune pits on mars. *J. Geopys. Res-Planet*, *123*(6), 1431-1448.

Elbelrhiti, H., Claudin, P., & Andreotti, B. (2005). Field evidence for surface-wave-induced instability of sand dunes. *Nature*, *437*(04058).

Ewing, R. C., Peyret, A.-P. B., Kocurek, G., & Bourke, M. (2010). Dune field pattern formation and recent transporting winds in the olympia undae dune field, north polar region of mars. *J. Geophys. Res.-Planet*, *115*(E8).

Feldman, W., Bourke, M., Elphic, R., Maurice, S., Bandfield, J., Prettyman, T., ... Lawrence, D. (2008). Hydrogen content of sand dunes within Olympia Undae.

Icarus, *196*(2), 422-432.

Finkel, H. J. (1959). The barchans of southern peru. *J. Geol.*, *67*(6), 614-647.

Groh, C., Rehberg, I., & Kruelle, C. A. (2011, Nov). Observation of density segregation inside migrating dunes. *Phys. Rev. E*, *84*, 050301(R). Retrieved from `https://link.aps.org/doi/10.1103/PhysRevE.84.050301` doi: 10.1103/PhysRevE.84.050301

Hansen, C., Byrne, S., Portyankina, G., Bourke, M., Dundas, C., McEwen, A., ... Thomas, N. (2013). Observations of the northern seasonal polar cap on Mars: I. Spring sublimation activity and processes. *Icarus*, *225*(2), 881-897.

Hansen, C. J., Bourke, M., Bridges, N. T., Byrne, S., Colon, C., Diniega, S., ... Thomas, N. (2011). Seasonal erosion and restoration of Mars' northern polar dunes. *Science*, *331*(6017), 575-578.

Herrmann, H. J., & Sauermann, G. (2000). The shape of dunes. *Physica A (Amsterdam)*, *283*, 24-30.

Hersen, P. (2004). On the crescentic shape of barchan dunes. *Eur. Phys. J. B*, *37*(4), 507–514.

Hersen, P., & Douady, S. (2005). Collision of barchan dunes as a mechanism of size regulation. *Geophys. Res. Lett.*, *32*(21).

Hersen, P., Douady, S., & Andreotti, B. (2002, Dec). Relevant length scale of barchan dunes. *Phys. Rev. Lett.*, *89*, 264301. Retrieved from `https://link.aps.org/doi/10.1103/PhysRevLett.89.264301` doi: 10.1103/PhysRevLett.89.264301

Hesp, P., & Hastings, K. (1998). Width, height and slope relationships and aerodynamic maintenance of barchans. *Geomorphology*, *22*, 193-204.

Kelley, D. H., & Ouellette, N. T. (2011). Using particle tracking to measure flow instabilities in an undergraduate laboratory experiment. *Am. J. Phys.*, *79*(3), 267-273.

Kleinhans, M. (2004). Sorting in grain flows at the lee side of dunes. *Earth-Science Reviews*, *65*(1), 75-102.

Long, J., & Sharp, R. (1964). Barchan-dune movement in imperiel valley, california. *Bull. Geol. Soc. Am.*, *75*, 149-156.

Makse, H. A. (2000). Grain segregation mechanism in aeolian sand ripples. *Eur. Phys. J. E*, *1*, 127-135.

Makse, H. A., Havlin, S., King, P. R., & Stanley, H. E. (1998). Experimental studies of stratification in a granular heleshaw cell. *Philos. Mag. B*, *77*(5), 1341-1351.

Norris, R. M. (1966). Barchan dunes of imperial valley, california. *J. Geol.*, *74*(3), 292-306.

Parteli, E. J. R., Durán, O., Bourke, M. C., Tsoar, H., Pöschel, T., & Herrmann, H. (2014). Origins of barchan dune asymmetry: Insights from numerical simulations. *Aeol. Res.*, *12*, 121–133.

Parteli, E. J. R., & Herrmann, H. J. (2007, Oct). Dune formation on the present mars. *Phys. Rev. E*, *76*, 041307. Retrieved from `https://link.aps.org/doi/10.1103/PhysRevE.76.041307` doi: 10.1103/PhysRevE.76.041307

Pommerol, A., Appr, T., Portyankina, G., Aye, K.-M., Thomas, N., & Hansen, C. (2013). Observations of the northern seasonal polar cap on Mars iii: CRISM/HiRISE observations of spring sublimation. *Icarus*, *225*(2), 911-922.

Portyankina, G., Pommerol, A., Aye, K.-M., Hansen, C. J., & Thomas, N. (2013). Observations of the northern seasonal polar cap on Mars ii: HiRISE photometric analysis of evolution of northern polar dunes in spring. *Icarus*, *225*(2), 898-910.

Rousseaux, G., Caps, H., & Wesfreid, J. (2004). Granular size segregation in underwater sand ripples. *Eur. Phys. J. E*, *13*, 213-219.

Runyon, K., Bridges, N., Ayoub, F., Newman, C., & Quade, J. (2017). An integrated model for dune morphology and sand fluxes on mars. *Earth Plan. Sci. Lett.*, *457*, 204 - 212.

Sauermann, C., Rognon, P., Poliakov, A., & Herrmann, H. J. (2000). The shape of the barchan dunes of Southern Morocco. *Geomorphology*, *36*, 47-62.
Schatz, V., Tsoar, H., Edgett, K. S., Parteli, E. J. R., & Herrmann, H. J. (2006). Evidence for indurated sand dunes in the martian north polar region. *J. Geopys. Res-Planet*, *111*(E4).
Schlichting, H. (2000). *Boundary-layer theory*. New York: Springer.
Vermeesch, P. (2011). Solitary wave behavior in sand dunes observed from space. *Geophys. Res. Lett.*, *38*(22).
Wenzel, J. L., & Franklin, E. M. (2019). Velocity fields and particle trajectories for bed load over subaqueous barchan dunes. *Granular Matter*, *21*, 321-334.
Yang, J., Dong, Z., Liu, Z., Shi, W., Chen, G., Shao, T., & Zeng, H. (2019). Migration of barchan dunes in the western quruq desert, northwestern china. *Earth Surf. Process. Landforms*, *44*(10), 2016-2029.